HHS Public Access

Author manuscript

Hepatology. Author manuscript; available in PMC 2024 November 01.

Published in final edited form as:

Hepatology. 2023 November 01; 78(5): 1462–1477. doi:10.1097/HEP.0000000000000420.

Purine anabolism creates therapeutic vulnerability in hepatocellular carcinoma via m^{6}A-mediated epitranscriptomic regulation

Man Hsin Hung[1], **Ching Wen Chang**[1,#], **Kathy Cheng Wang**[1], **Jittiporn Chaisaingmongkol**[2,3], **Mathuros Ruchirawat**[2,3], **Tim F. Greten**[4,5], **Xin Wei Wang**[1,5,6,*]

[1]Laboratory of Human Carcinogenesis, Center for Cancer Research, National Cancer Institute, Bethesda, MD 20892, USA

[2]Laboratory of Chemical Carcinogenesis, Chulabhorn Research Institute, Bangkok 10210, Thailand

[3]Center of Excellence on Environmental Health and Toxicology (EHT), OPS, MHESI, Thailand

[4]Thoracic and Gastrointestinal Oncology Branch, Center for Cancer Research, National Cancer Institute, National Institutes of Health, Bethesda, MD 20892, USA.

[5]Liver Cancer Program, Center for Cancer Research, National Cancer Institute, Bethesda, MD 20892, USA

[6]Lead contact

Abstract

Background and Aims—Purines are building blocks for cellular genome and excessive purine nucleotides are seen in tumors. However, how purine metabolism is dysregulated in tumor and impacting tumorigenesis remains elusive.

Approach and Results—Transcriptomic and metabolomic analysis of purine biosynthesis and purine degradation pathways were performed in the tumor and associated non-tumor liver tissues obtained from 62 patients with hepatocellular carcinoma (HCC), one of the most lethal cancers worldwide. We found that most genes in purine synthesis are upregulated while genes in purine degradation are inhibited in HCC tumors. High purine anabolism is associated with unique somatic mutational signatures linked to patient prognosis. Mechanistically, we discover that increasing purine anabolism promotes epitranscriptomic dysregulation of DDR machinery through upregulating RNA N6-methyladenosine modification. High purine anabolic HCC is sensitive to DDR-targeting agents but not to standard HCC treatments, correlating with the clinical outcomes in five independent HCC cohorts containing 724 patients. We further showed that high purine

*Correspondence: xw3u@nih.gov.

#Current address: Graduate Institute of Metabolism and Obesity Sciences, Taipei Medical University, Taipei 110301, Taiwan

AUTHOR CONTRIBUTIONS

M.H.H. and X.W.W. developed study concept and directed experimental design; M.H.H. performed computational analysis; M.H.H., C.W.C, K.C.W, T.F.G, J.C., and M.R. conducted experiments and additional data analysis; M.H.H. and X.W.W. wrote the manuscript. All authors read, edited, and approved the manuscript.

DECLARATION OF INTERESTS

The authors declare no competing interests.

anabolism determines the sensitivity to DDR-targeting agents in 5 HCC cell lines *in vitro* and *in vivo*.

Conclusion—Our results reveal a central role of purine anabolism in regulating DDR, which could be therapeutically exploited in HCC.

Graphical Abstract

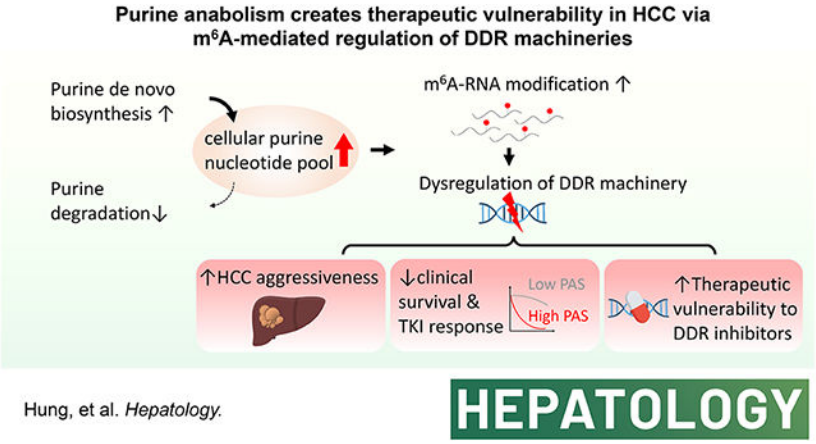

Keywords

Purine metabolism; therapeutic vulnerability; DNA damage repair; reprogramming; N6-methyladenosine; epitranscriptomic; DTL; hepatocellular carcinoma; berzosertib

Introduction

Purines, including adenine and guanine, are the most abundant metabolites in a mammalian cell, crucial for constructing genome, providing cellular energy, and intracellular signaling[1, 2]. The cellular purine nucleotide pool is maintained by a coordinated action of the *de novo* purine biosynthesis, purine salvage pathway, and purine degradation pathway. Tumors are known to contain a larger purine nucleotide pool compared to normal cells, and activation of purine biosynthesis has been shown in various types of malignant diseases[2, 3]. However, how different parts of purine metabolism integrated in tumors to support tumor fitness has not been well defined.

Hepatocellular carcinoma (HCC) is the most prevalent primary liver cancer with high mortality and limited treatment for advanced disease[4]. Ma et al. recently demonstrated that inactivation of *de novo* purine biosynthesis mediates the function of a tumor suppressor, dual-specificity tyrosine (Y) phosphorylation-regulated kinase 3, in HCC[5]. Another study by Chong et al. revealed that activation of Phosphoinositide 3 kinase signaling may promote the upregulation of *de novo* purine biosynthesis in HCC, and targeting inosine-5'-monophosphate dehydrogenase (IMPDH), a key enzyme of *de novo* purine biosynthesis, could significantly inhibit HCC tumor growth[6]. However, there is a lack of knowledge on the functional status of global purine metabolism in HCC and how various purine metabolic pathways collectively coordinate together to drive HCC fitness and therapeutic response.

Here, we aimed to explore the roles of purine metabolism in HCC by applying integrative genomic, transcriptomic, and metabolomic profiles of HCC tumors and associated non-tumor tissues. We show that a tumor-specific activation of purine anabolism promotes the dysregulation of DNA damage repairing (DDR) machinery in HCC, creating a therapeutic vulnerability of HCC to DDR targeting agents. Our results suggest that targeting DDR may represent as attractive strategies in patients with high purine anabolic HCCs, and purine anabolic status could be a valuable biomarker to allocate systemic treatments for patients with advanced HCC.

MATERIALS AND METHODS

HCC cohorts

We identified 62 HCC samples and 59 associated non-tumor liver tissues of TIGER-LC cohort (GSE76297) [7] as discovery cohort, and the transcriptome data obtained from 756 bulk tumor and 289 associated non-tumor tissues from 5 independent cohorts and single cell transcriptome data from and 16 HCC patients received immune checkpoint inhibitor (GSE 151530)[8] as validation cohorts.

Animal Study

Six-week-old male NOD/SCID mice obtained from NCI/Frederick (Frederick, MD, USA) were used in this study. All mice were group-housed (5 mice per cage) and maintained under a regular light-dark cycle altered every 12 hours with free access to water and standard mouse chow. Huh7 cell was examined regularly for Mycoplasma prior tumor implantation. The animal study protocol (LHC-001-4) was reviewed and approved by the National Cancer Institute-Bethesda Animal Care and Use Committee (Bethesda, MD, USA).

For subcutaneous tumorigenic studies, $1x10^6$ Huh7 cells stably transduced with lenti-SpCas9-2A-Puro (empty vector) or lenti-SpCas9-2A-Puro-ATIC were mixed in 100 μL of a 1:1 solution of Matrigel (Corning) and DMEM (Thermo Fisher) and injected subcutaneously into bilateral flank of the mice. For treatment response experiment, Huh7 cells were treated with berzosertib (Selleckchem, Cat.# S7102) 5 μM or mock for 48 hours and harvested. Cell were trypan blue counted and $1x10^6$ viable berzosertib-treated or mock-treated Huh7 cells were mixed with Matrigel using the above-mentioned formula and subcutaneously injected into the flank of mice. Tumor growth was then measured regularly until euthanasia. Tumors were obtained after euthanasia and fixed with 10% formalin overnight and transferred to 70% ethanol prior to paraffin embedding.

Quantification and statistical analysis

Statistical significance between two groups was determined using an unpaired Student's t-test for normally distributed data, and non-parametric Mann-Whitney U-test for non-normally distributed data, and ANOVA test was used for a comparison between three or more groups. The relationship between two features were examined using Pearson correlation test. Survival data was analyzed using Kaplan-Meier survival analysis with a *p* value generated by the Cox-Mental log-rank test. All the in vitro experiments were examined by biologically independent triplicates. All data were presented as mean ±

standard error of at least three independent experiments. The statistics tests were executed using GraphPad Prism V7.0. unless otherwise specified. All *p* values presented were two-sided and a *p* value less than 0.05 was considered as statistically significant.

More detail about the clinical cohorts included in this study, bioinformatic study and *in vitro* and *in vivo* experiments are described in the Supporting Materials and Supplementary Figure 1.

Results

Contrasting changes of purine synthesis and its degradation contributes to high purine anabolism in HCC

To gain insights into HCC remodeling of purine metabolism, we performed metabolomic and transcriptomic profiling of purine metabolic pathways on 62 clinical HCC tumor and paired non-tumor tissues (TIGER-LC cohort)[7]. The levels of genes and metabolites related to purine synthesis, particularly the *de novo* biosynthesis, were significantly higher in HCC tumors compared to non-tumor liver tissues, while an opposite trend was observed in genes and metabolites related to purine degradation (Fig. 1a-b and Supplementary Fig. 2a). We found a negative correlation between purine *de novo* biosynthesis and purine degradation in HCC tumor tissues but not in non-tumor tissues (Fig. 1c), while comparable changes in pyrimidine metabolism was not observed (Supplementary Fig. 2a-b). Notably, we observed consistent purine metabolic changes in an independent HCC cohort, TCGA-LIHC (n=366, Supplementary Fig. 3a-b). To determine how different parts of purine metabolism relate with HCC fitness, we obtained the Gene Essentiality score (Chronos score) from the Cancer Dependency Map[9, 10]. We observed a pattern of decreasing Chronos score from purine catabolic genes to purine anabolic genes among 22 HCC cell lines (Fig. 1d), suggesting an increasing dependency of purine anabolism in HCC.

Next, we analyzed the mutation, somatic copy number alterations (SCNA) and DNA methylation profiles to identify molecular mechanism driving purine metabolic changes in HCC. We found that somatic mutations in the purine metabolic genes are very rare in HCC tumors, but several genes within purine *de novo* biosynthesis and salvage pathways showed a strong association between SCNA and their mRNA levels (Supplementary Fig. 4a). Meanwhile, the expression levels of genes within purine degradation pathway correlates with the promoter DNA methylation status (Supplementary Fig. 4a). Importantly, the distribution of these significant molecular alterations correlated with the activity of purine anabolism in HCC (Supplementary Fig. 4b-c). These results are consistent with the hypothesis that activation of purine anabolism in HCC may be induced by both SCNA and DNA methylation of key genes in the purine metabolism pathways.

Among all purine metabolic genes, we bioinformatically selected GMPS and XDH based on the performance to differentiate tumors from non-tumor liver tissues in TIGER-LC cohort (Fig. 1e and Supplementary Table 1) and constructed the purine anabolism score (PAS) based on the standardized expression difference of GMPS and XDH. We validated the utility of PAS on capturing the transcriptomic and metabolomic changes of purine metabolism in both TIGER-LC cohort (the training set, Fig. 1f and Supplement Fig. 5a-b) and TCGA-

LIHC cohort (the validation set, Supplement Fig. 5c-d). Patients with high PAS HCCs were associated with higher AFP, worse tumor differentiation and adverse overall survival (Supplementary Table 2, Fig. 1g and Supplementary Fig. 3c). Among common HCC-related etiologies, we observed a consistent increase of PAS in HCC tumors compared to non-tumor tissues (Supplementary Fig. 3d). To determine whether purine anabolism affected HCC mutation, we examined exome sequencing data of HCC in TIGER-LC and TCGA-LIHC cohorts. High PAS HCCs were significantly enriched with C>A and C>G substitution, while A>G, and A>T substitution were more likely to be observed in tumors with low PAS (Fig. 1h and Supplementary Fig. 3e). Furthermore, mutations in the high PAS tumors occurred significantly more on the transcribed strands than the non-transcribed strands, indicating the presence of transcription-associated mutation strand bias (Fig. 1i and Supplementary Fig. 6). Interestingly, using a method to measure intratumor genomic heterogeneity (ITH)[11], we found that tumors with high PAS had a significantly higher levels of ITH compared to tumors with low PAS (Fig. 1j and Supplementary Fig. 3f). Collectively, these results indicate that aberrant activation of purine anabolism in HCC is associated with types of mutations, intratumor genomic heterogeneity and adverse clinical outcome in HCC patients.

Aberrant activation of purine anabolism induces dysregulation of DDR machinery via m^{6}A-associated epitranscriptomic control

To understand how activation of purine anabolism affects HCC biology, we performed pathway analysis and found a significant enrichment of DDR pathway in high PAS tumors, suggesting that activation of purine anabolism may induce genomic instability via promoting DDR dysregulation (Fig. 2a and Supplementary Table 3). Mutation of DDR genes is a common cause of DDR dysfunction in cancer[12], but we did not observe specific enrichment of mutations of key DDR genes in HCC tumors in TIGER-LC and TCGA-LIHC cohort (Supplementary Table 4). Therefore, we profiled the transcriptome changes of 409 DDR-related genes in HCC. Using unsupervised hierarchical clustering, we found that HCC patients formed two major patient clusters, and, notably, there was a great degree of overlapping between purine-anabolism-defined and DDR-defined tumor classes (Fig. 2b). DDR2 tumors, which exerted higher ITH and worse survival (Fig. 2c-d) compared to DDR1 tumor, was preferentially enriched in high PAS tumors (Supplementary Fig. 7a). The correlation of PAS and DDR genes was consistently observed in HCC tumor and non-tumor tissues, linking to tissue malignancy and patients' clinical outcome, but such relationship was not seen with tumor pyrimidine anabolism (Supplementary Fig. 7b-e). Furthermore, we examined enrichment of individual DDR pathways and found that high PAS tumors were significantly enriched for double strand break repairing pathways but were depleted for the nucleotide excision repair pathway (Supplementary Fig. 7f). We analyzed purine metabolites associated with the purine anabolic status and DDR status in TIGER-LC cohort. Five out of 35 purine metabolites, including 7-methylguanine, N6-methyladenosine (m^{6}A), N2,N2-dimethylguanosine, N2-methylguanosine, and N6-carbamoylthreonyladenosine, were significantly enriched in the high PAS tumors and DDR2 tumors (Fig. 2e). Interestingly, these identified metabolites are modified purine nucleobases commonly present as RNA modifications[13-15], and most of them do not have a well-defined function. We focused on m^{6}A because it is the most abundant post-transcriptional RNA modification in eukaryotic mRNAs and have been shown

to exhibit broad impacts on gene expression[15]. We hypothesized that purine anabolism may preferentially induce DDR dysregulation via m^{6}A-mediated activities in HCC. We obtained human m^{6}A-associationed epitranscriptome from WHISTLE, a machine learning framework that indicated 9,941 predicted m^{6}A sites across genome[16]. By analyzing the presence of m^{6}A-sites among 8 different cancer hallmarks, we found that the DDR pathway contained the highest percentage of genes with potential m^{6}A site (Fig. 2f), suggesting that the change in m^{6}A abundance may preferentially affect the DDR machinery. We next analyzed m^{6}A regulatory genes and found that the expressions of m^{6}A writer and m^{6}A reader genes increased with the level of m^{6}A in HCC tumors, suggesting that the m^{6}A level characterized by metabolomic analysis reflects the level of m^{6}A on RNAs (Supplementary Figure 8a). Furthermore, we observed a collective upregulation of m^{6}A writer and m^{6}A reader genes in high PAS HCC and DDR2 tumors, and the levels of PAS and m^{6}A regulatory genes were significantly corrected with PCNA expression (Supplementary Fig. 8b-d), indicating strong associations between purine anabolism, m^{6}A activities and HCC proliferation. Next, we identified DTL, a substrate receptor associated with Cullin4-ring E3 ubiquitin ligase complex[17], as potential downstream of purine anabolism/m^{6}A by the presence of high number of m^{6}A sites and its expression showing the highest change with the tumor DDR status (Fig. 2g). DTL expression was significantly elevated in HCC tumors and was positively associated with PAS (Fig. 2h-i). Consistently, high DTL tumors were enriched comparable mutational alterations and adverse clinical outcomes observed in high PAS tumor (Fig. 2j-l). Together, our data support the model that activation of purine anabolism promotes m^{6}A -mediated remodeling of DDR, causing upregulation of DTL and increasing genomic complexity in HCC.

HCC with high purine anabolism acquires therapeutic vulnerability

Next, we asked how the purine anabolism affect therapeutic vulnerability in HCC. We obtained drug response data of 11 HCC cell lines to 180 anti-cancer therapeutics from the Genomics of Drug Sensitivity in Cancer database[18]. We performed correlation analysis between nucleotide anabolism and drug sensitivity across all HCC cells and summarized the distribution of correlation coefficient in Figure 3a (Supplementary Table 5). For DDR-targeting drugs, we observed a bimodal distribution of the correlation coefficient between purine anabolism and drug sensitivity, where a higher peak occurring at the range between −0.2 - −0.8, suggesting that high purine anabolism links to better anti-HCC response in most of the DDR-targeting drugs (Fig. 3a, left upper panel). In contrast, the correlation coefficient of purine anabolism and the sensitivity to non-DDR-targeting drugs showed a unimodal distribution with the peak shift to the right, suggesting that HCC cells with high purine anabolism are resistant to non-DDR-targeting compounds (Fig. 3a, left lower panel). As a control, we examined the relationship between pyrimidine anabolism and drug response and found no comparable pattern as purine anabolism (Fig. 3a, right panel). To further test such effect, we examined the relationship of PAS and molecular signatures related to therapeutic responses in HCC tumors[19-22] (Supplementary Table 6). As shown in Fig. 3b, tumor PAS and DTL level were positively correlated with response to DDR-targeting therapies, namely berzosertib (a specific ATR inhibitor) and radiotherapy (a therapeutic modality that directly induces DNA breaks), while showing negative or no correlation with the responsiveness of sorafenib anti-Programmed Cell Death Protein 1 (PD1) therapy.

Sorafenib and anti-PD1 monoclonal antibodies are approved treatments for patients with advanced HCC, and DDR-targeting chemotherapies are commonly administrated as transarterial chemoembolization (TACE) to HCC patients[23, 24]. To validate the clinical relevance of our findings, we analyzed tumor transcriptomic data and clinical outcomes with corresponding treatments from five independent HCC cohorts (Supplementary Fig. 1). The first cohort included 75 HCC patients received a combination of DDR-targeting chemotherapies, including cisplatin, fluorouracil and mitomycin C, as preventative TACE and 142 patients received conservative observation after curative surgical tumor resection[25, 26]. Among patients receiving preventative TACE, the average PAS in patients who did not have tumor relapse after surgery and TACE was significantly higher than patients who developed recurrence of tumor, but tumor PAS was not associated with the clinical outcomes of patients without TACE (Fig. 3c). In 60 patients harboring advanced HCC (BCLC stage>0 & TNM > T1 or CLIP score >1), we observed a significant survival benefit of TACE treatment in patients with high tumor PAS (p=0.0064), but not in patients with low tumor PAS (p=0.5873, Fig. 3d). Consistently, we observed a similar predictive effects of tumor PAS on the benefit of TACE for advanced HCC patients in an independent Korean cohort (Fig. 3e). Intriguingly, in the three other HCC cohorts testing sorafenib[21, 27] and anti-PD1 therapy[8], high purine anabolism was inversely linked with treatment response and clinical survival advantage (Fig. 3f-g). Together, our data suggests a role of tumor purine anabolism in modulating therapeutic vulnerability in HCC, and high purine anabolic tumor is more susceptible to DDR-targeting treatment, such as ATR inhibitor berzosertib, than current standard HCC treatments.

Purine anabolism determines hepatocarcinogenesis and cellular DNA damage by upregulating m^{6}A/DTL

To experimentally validate the role of tumor purine anabolism in affecting tumorigenesis and therapeutic vulnerability of HCC, we used the clustered regularly interspaced short palindromic repeats (CRISPR)-Cas9 system to delete ATIC, a key enzyme in *de novo* purine biosynthesis, in Huh1 and Huh7, two HCC cell lines with high purine anabolism (Fig. 4a and 6a). We used the quantitative polymerase chain reaction and enzyme-linked immunosorbent assay (ELISA) and validated that ATIC downstream genes, namely *GMPS*, *IMPDH2,* and purine biosynthesis product, cGMP, were significantly reduced in ATIC-knockout (KO) cells (Fig. 4b). We found that deletion of ATIC significantly inhibited the proliferation and colony formation of Huh1 and Huh7 cells, which were reversed by supplementing exogenous nucleosides (Fig. 4c-d). In addition, we ectopically overexpressed (OE) ATIC in SNU475 cells, an HCC cell line with a relatively lower purine anabolism, and found that ATIC-OE significantly increased purine metabolism and cell growth of SNU475 cell (Fig. 4e). Next, we studied the level of cellular DNA damage by examining 8-hydroxy-2'-deoxyguanosine (8-OHdG) and r-H2AX in Huh7 and SNU475 cells. As shown in Fig. 4f, the degree of DNA damage was significantly reduced in Huh7 cells with ATIC-KO, while nucleoside supplement counteracted with such effects. Conversely, the levels of DNA damage markers were significantly elevated in SNU475 cells with ATIC-OE in comparison to control SNU475 cells (Fig. 4g). We utilized an Huh7 subcutaneous xenografted tumor model used in our previous study [28] to further examine the effects of ATIC on *in vivo* tumor growth. As shown in Fig. 4h, ATIC-KO significantly reduced the

growth of Huh7 tumor (n=8, p=0.00026) and decreased the expressions of Ki-67 (p=0.0129) and r-H2AX (p=0.0031) in tumors.

Next, we tested whether purine anabolism regulate m^{6}A in HCC. We determined the level of m^{6}A on RNA using ELISA. In both Huh1 and Huh7 cells, the levels of m^{6}A had a 50%-75% reduction in ATIC-KO cells compared to the control cells (Fig. 5a), while the pool nucleosides supplement conversely increased the m^{6}A level of the ATIC-KO cells in a dose-dependent manner (Fig. 5c). Consistently, the ATIC-OE SNU475 cells presented significant higher levels of m^{6}A (Fig. 5b). Furthermore, we found that ATIC-KO cells had significantly lower expressions of m^{6}A regulatory genes, while an opposite change was observed in ATIC-OE cells (Supplementary Fig. 9a-b). To confirm the specificity of purine anabolism in controlling the m^{6}A level, we treated cells with purine and pyrimidine nucleosides separately. As shown in Fig. 5d, only supplement of adenosine and guanosine, not pyrimidine nucleosides, increased the m^{6}A level in ATIC-KO Huh1 cells.

We assessed whether DTL is controlled by purine anabolism/m^{6}A. Consistent with the changes of m^{6}A, the expressions of DTL in ATIC-KO Huh1 or Huh7 cells showed significant reduction compared to control cells, which was reversed by the nucleoside supplement (Fig. 5e-f). Meanwhile, the level of DTL showed a 1.3-fold increase in the ATIC-OE SNU475 cells (Fig. 5g). Consistently, we found a significant downregulation of DTL and decreased cell proliferation and colony formation were accompanied by inhibition of METTL3 in the siMETTL3-transfected Huh1 and Huh7 cells (Fig. 5h and Supplementary Fig. 9c-f). Since m^{6}A modification regulates RNA stability [15], we examined whether purine anabolism/m^{6}A affects the stability of DTL. In comparison to control cells, the expression of DTL decayed significantly faster in ATIC-KO Huh1 cells after the treatment of a transcription inhibitor, actinomycin D, while an opposite change was observed in ATIC-OE SNU475 cells (Fig. 5i). Consistently, Huh1 and Huh7 cells with knockdown of DTL showed a significant inhibition of *in vitro* cell proliferation, while SNU475 cell with ectopic OE of DTL exerted a nearly two-fold increase of cell proliferation (Fig. 5j-k and Supplementary Fig. 9g). DTL-KO significantly inhibited the levels of 8-OHdG and r-H2AX in Huh7 cells, while DTL-OE significantly elevated these DNA damage markers in SNU475 cells (Fig. 5l-m). Together, our data support the model that purine anabolism promotes HCC growth and DDR dysfunction through upregulating m^{6}A /DTL.

Purine anabolism impacts the treatment response of HCC cells to DDR-targeted agents

To experimentally examine the link between purine anabolism and therapeutic susceptibility in HCC, we treated five HCC cells lines with two approved HCC target therapies and eight compounds targeting various DDR pathways. As shown in Figure 6a, therapeutic responses were greatly affected by purine anabolic activities of HCC cells. For sorafenib and regorafenib, SNU475, the cell line that has the lowest purine anabolism, shows a lower IC_{50} than that of the other four HCC cells with higher purine anabolism. For agents that inhibit the repairing of or cause double strand DNA breaks, namely berzosertib, mitoxantrone, doxorubicin and paclitaxel, we found that HCC cells with high purine anabolism were more sensitive to these compounds in comparison to sorafenib and regorafenib, while SNU475 cells showed a high resistance to such treatments. For compounds that primarily target single

strand break repair pathways, including olaparib, talazoparib, veliparib and methoxyamine, none caused significant cytotoxic effects up to 10 μM in all the HCC cell lines we tested. We then focused on berzosertib and investigated whether the cytotoxic differences between different HCC cell lines correlated with the degree of DNA damage. As shown in Fig. 6b, berzosertib induced a dose dependent upregulation of r-H2AX signaling in Huh1, Huh7 and Hep3B cells, while such effect was not observed in SNU475 cells. Next, we tested whether purine anabolism modulated the effects of berzosertib in HCC. In Huh7 cells, ATIC-KO attenuated the cytotoxic effects of berzosertib, which was counteracted by nucleoside supplement (Fig. 6c, left panel). Consistently, the ATIC-OE SNU475 cells or SNU475 cells treated with exogeneous nucleosides presented with a significant higher level of berzosertib-induced cytotoxicity as compared to control (Fig. 6c, right panel). Consistently, berzosertib treatment induced a dose-dependent increase of apoptotic cells in Huh7 cells, while such effect was decreased in ATIC-KO Huh7 cells (Fig. 6d, upper panel). In SNU475 cells, berzosertib treatment showed little pro-apoptotic effects, while ATIC-OE conversely increased the level of berzosertib-induced cell apoptosis (Fig. 6d, lower panel). Furthermore, we found that inhibition of DTL attenuates the berzosertib-induced cytotoxic effect and ectopic expression of DTL conversely enhanced it in HCC cells (Fig. 6e). Consistently, we found that berzosertib treatment significantly inhibits *in vivo* tumor growth in the Huh7 xenograft HCC model (Fig. 6f). After three weeks, only one out of eight berzosertib-treated Huh7 cells established tumor *in vivo*, while all the vehicle-treated tumors developed successfully (p=0.0014). Furthermore, the sizes of Huh7 tumor in berzosertib treatment arm were significantly smaller compared to the control tumors (p=0.0007). In summary, our data indicates that high purine anabolism/DTL creates therapeutic vulnerability to double strand DNA break repair inhibitor, like berzosertib, in HCC.

Discussion

In this study, we demonstrated the changes of purine synthesis and purine degradation occur jointly in HCC, thereby creating a high purine anabolism linking to dysregulation of DDR and genomic instability in tumors. We revealed that the basis for DDR remodeling induced by purine anabolism in HCC is through m^6A-associated epitranscriptomic control on m^6A+ DDR genes. This feature allowed us to link HCC with high purine anabolism and a therapeutic vulnerability to DDR-targeting agents, while showing resistance to standard treatments for advanced HCC, such as sorafenib.

Dysregulation of DDR is a common feature observed in cancer which enable cancer cells to accumulate genomic changes that contribute to their aggressiveness[12]. For HCC, multiple HCC-associated risk factors were shown to promote the occurrence of DNA damage[29], and transcriptomic changes of DDR genes were linked with aggressive clinical behavior and therapeutic resistance [30]. Intriguingly, the incidences of pathological genetic alterations commonly account for DDR dysfunction, such as mutation of *BRCA1/2* and microsatellite instability-high status, were much lower in HCC than that observed in other major types of cancer[31, 32], suggesting the presence of additional mechanisms responsible for the alteration of DDR machinery in HCC. In the present work, we revealed a new role of purine metabolic alteration in promoting DDR dysregulation via a m^6A-associated mechanism. High purine anabolism led to consistent transcriptomic changes of DDR genes in both

tumor and associated non-tumor tissues, suggesting that such DDR dysregulation induced by purine anabolism is independent from oncogenic mutation and could happen during early hepatocarcinogenesis. Literature shows that aberration of m^{6}A-RNA and m^{6}A-regulatory genes are positively associated with tumor mutation burden and genomic instability in HCC and other malignancies[33, 34]. Consistent with previous publications, we found that upregulation of m^{6}A and m^{6}A regulatory genes in HCC are significantly associated with transcriptomic reprograming of DDR pathways and genomic instability. Importantly, we show that the m^{6}A-associated machinery is specifically regulated by purine, not pyrimidine, anabolism. Our result may help to explain the findings by Darè et al. that accumulation of purine nucleotide was more mutagenic than pyrimidine nucleotide[35] and the observations made by Zhou et al. that only the *de novo* synthesis of purine, not pyridmidine, regulated DNA repair in glioblastoma[36]. It is worth noticing that the levels of m^{6}A in clinical HCC tumors reported in current study were determined by metabolomic analysis. Though there is no literature directly compares such method with the level of m^{6}A on RNAs in clinical samples, we found that the metabolomic level of m^{6}A linked significantly with the expression of m^{6}A regulatory genes, which are known to recognize and function on specific RNA motif, in HCC tumors, suggesting that the metabolomic analysis on m^{6}A may reflect the changes relevant to RNAs. Further studies are needed to validate the utility of metabolomic studies in characterizing m^{6}A-RNA modifications in clinical samples.

Dysregulation of DDR in cancer often leads to a reduced repertoire of DDR capability compared with normal cells, which consequently makes cancer cells reliant on a subset of repair pathways and to be more susceptible to DDR inhibitors targeting those pathways[37]. In this study, we showed that high purine anabolic HCCs exert a preferential activation of double strand break repair pathways and are more sensitive to compounds that inhibits these pathways. Miller et al. analyzed the metabolomic changes of 36 non-small cell lung cancer patients and found that upregulation of purine metabolism is one of the most dominate changes associated better response to DNA damaging chemotherapies[38]. Meanwhile, purine metabolism was found to regulate DDR pathways in glioblastoma, but activation of purine *de novo* pathway conveys resistance to radiotherapy and a DNA targeting chemotherapy, temozolomide[36]. According to a systemic analysis performed in The Cancer Genome Atlas, HCC and glioblastoma exert distinct molecular background regarding DDR pathways[31], which may explain why purine anabolism shows different effects on tumor susceptibility to DDR damaging treatments in these two tumors. In present study, we show the pre-clinical effects of berzosertib in HCC. Berzosertib is a potent and specific ATR inhibitor that is currently under active early phase clinical testing [39]. Though there is no clinical trial designed to examine the effects of berzosertib in HCC patients yet, published data of using berzosertib as monotherapy or in combination with other treatments indicates that it is well-tolerated and has synergistic effects with cisplatin, gemcitabine and other DNA damaging drugs in various types of solid tumors[40]. Further studies are needed to evaluate the clinical benefit of berzosertib and the utility of purine anabolic genes to predict berzosertib treatment response in HCC patients.

Additionally, we showed that that high tumor purine anabolism associated with clinical benefit of DNA-break-inducing chemotherapies given as preventative TACE in patients with intermediate to high risk HCCs. Post-operative preventative (or adjuvant) TACE is

a procedure that had been actively tested in various clinical trials aiming to decrease the recurrence rate of HCC after curative tumor resection [25, 41] and positive clinical benefit of such measurement in patients with intermediate or high risks of HCC recurrence was suggested by several randomized clinical trials [41]. The therapeutic vulnerabilities of high purine anabolic HCCs to chemotherapies that induce double strand DNA breaks showed in our study suggested a potential use of purine anabolism as a biomarker to predict the clinical benefit of adjuvant TACE. Nevertheless, TACE is a highly heterogenous procedure in terms of regiment and the biological effects of TACE are not limited to induction of DNA damage, which may influence the ability of purine anabolism to predict the clinical benefits of TACE. Further studies are needed to examine whether purine anabolism also influences TACE through other mechanisms and whether purine anabolism could be used to predict the clinical benefit of TACE in other clinical setting.

In summary, we have defined activation of purine anabolism as a key driver for DDR dysregulation and disclose its impact on therapeutic vulnerability in HCC. These results have motivated further studies to test the utility of DDR inhibitors, like berzosertib, for the treatment of HCC with high purine anabolism and the synergistic effects of inhibiting purine anabolism with sorafenib or immune checkpoint inhibitors for patients with HCC.

Supplementary Material

Refer to Web version on PubMed Central for supplementary material.

Acknowledgement

We thanked the editorial assistance provided by the NIH Fellows Editorial Board.

Financial support and sponsorship

This work was supported by the intramural research program of the Center for Cancer Research National Cancer Institute of the United States (grant number ZIA BC 010877, ZIA BC 010876, ZIA BC 010313 and ZIA BC 011870).

List of Abbreviations

8-OHdG	8-hydroxy-2’-deoxyguanosine
CRISPR	clustered regularly interspaced short palindromic repeats
DDR	DNA damage repairing
ELISA	enzyme-linked immunosorbent assay
HCC	Hepatocellular carcinoma
IMPDH	inosine-5’-monophosphate dehydrogenase
ITH	intratumor genomic heterogeneity
IQR	interquartile range
KO	knockout

m^6A	N6-methyladenosine
OE	overexpressed
PAS	purine anabolism score
SCNA	somatic copy number alterations
TACE	transarterial chemoembolization

REFERENCES

1. Pedley AM, Benkovic SJ. A New View into the Regulation of Purine Metabolism: The Purinosome. Trends Biochem Sci. Feb 2017;42(2):141–154. doi:10.1016/j.tibs.2016.09.009 [PubMed: 28029518]
2. Vander Heiden MG, DeBerardinis RJ. Understanding the Intersections between Metabolism and Cancer Biology. Cell. 2017/02/09/ 2017;168(4):657–669. doi:10.1016/j.cell.2016.12.039 [PubMed: 28187287]
3. Traut TW. Physiological concentrations of purines and pyrimidines. Molecular and Cellular Biochemistry. 1994/11/01 1994;140(1):1–22. doi:10.1007/BF00928361 [PubMed: 7877593]
4. Villanueva A Hepatocellular Carcinoma. The New England Journal of Medicine. 2019;380(15):1450–1462. doi:10.1056/NEJMra1713263 [PubMed: 30970190]
5. Ma F, Zhu Y, Liu X, et al. Dual-Specificity Tyrosine Phosphorylation-Regulated Kinase 3 Loss Activates Purine Metabolism and Promotes Hepatocellular Carcinoma Progression. Hepatology. Nov 2019;70(5):1785–1803. doi:10.1002/hep.30703 [PubMed: 31066068]
6. Chong YC, Toh TB, Chan Z, et al. Targeted Inhibition of Purine Metabolism Is Effective in Suppressing Hepatocellular Carcinoma Progression. Hepatology Communications. 2020;4(9):1362–1381. doi:10.1002/hep4.1559 [PubMed: 32923839]
7. Chaisaingmongkol J, Budhu A, Dang H, et al. Common Molecular Subtypes Among Asian Hepatocellular Carcinoma and Cholangiocarcinoma. Cancer Cell. Jul 10 2017;32(1):57–70 e3. doi:10.1016/j.ccell.2017.05.009 [PubMed: 28648284]
8. Ma L, Wang L, Khatib SA, et al. Single-cell atlas of tumor cell evolution in response to therapy in hepatocellular carcinoma and intrahepatic cholangiocarcinoma. J Hepatol. Jun 30 2021;75:1397–1408. doi:10.1016/j.jhep.2021.06.028 [PubMed: 34216724]
9. Tsherniak A, Vazquez F, Montgomery PG, et al. Defining a Cancer Dependency Map. Cell. Jul 27 2017;170(3):564–576.e16. doi:10.1016/j.cell.2017.06.010 [PubMed: 28753430]
10. Dempster JM, Rossen J, Kazachkova M, et al. Extracting Biological Insights from the Project Achilles Genome-Scale CRISPR Screens in Cancer Cell Lines. bioRxiv. 2019:720243. doi:10.1101/720243
11. Kwon SM, Budhu A, Woo HG, et al. Functional Genomic Complexity Defines Intratumor Heterogeneity and Tumor Aggressiveness in Liver Cancer. Scientific Reports. 2019/11/15 2019;9(1):16930. doi:10.1038/s41598-019-52578-8 [PubMed: 31729408]
12. Dietlein F, Thelen L, Reinhardt HC. Cancer-specific defects in DNA repair pathways as targets for personalized therapeutic approaches. Trends in Genetics. 2014;30(8):326–339. doi:10.1016/j.tig.2014.06.003 [PubMed: 25017190]
13. Luo Y, Yao Y, Wu P, Zi X, Sun N, He J. The potential role of N(7)-methylguanosine (m7G) in cancer. J Hematol Oncol. May 19 2022;15(1):63. doi:10.1186/s13045-022-01285-5 [PubMed: 35590385]
14. Chen W, Song X, Lv H, Lin H. iRNA-m2G: Identifying N^2-methylguanosine Sites Based on Sequence-Derived Information. Molecular Therapy - Nucleic Acids. 2019;18:253–258. doi:10.1016/j.omtn.2019.08.023 [PubMed: 31581049]
15. Barbieri I, Kouzarides T. Role of RNA modifications in cancer. Nature Reviews Cancer. 2020/06/01 2020;20(6):303–322. doi:10.1038/s41568-020-0253-2 [PubMed: 32300195]

16. Chen K, Wei Z, Zhang Q, et al. WHISTLE: a high-accuracy map of the human N6-methyladenosine (m6A) epitranscriptome predicted using a machine learning approach. Nucleic Acids Research. 2019;47(7):e41–e41. doi:10.1093/nar/gkz074 [PubMed: 30993345]
17. Panagopoulos A, Taraviras S, Nishitani H, Lygerou Z. CRL4(Cdt2): Coupling Genome Stability to Ubiquitination. Trends Cell Biol. Apr 2020;30(4):290–302. doi:10.1016/j.tcb.2020.01.005 [PubMed: 32044173]
18. Yang W, Soares J, Greninger P, et al. Genomics of Drug Sensitivity in Cancer (GDSC): a resource for therapeutic biomarker discovery in cancer cells. Nucleic Acids Research. 2012;41(D1):D955–D961. doi:10.1093/nar/gks1111 [PubMed: 23180760]
19. Sun Z, Wang X, Wang J, et al. Key radioresistance regulation models and marker genes identified by integrated transcriptome analysis in nasopharyngeal carcinoma. Cancer Med. Oct 2021;10(20):7404–7417. doi:10.1002/cam4.4228 [PubMed: 34432380]
20. Thomas A, Takahashi N, Rajapakse VN, et al. Therapeutic targeting of ATR yields durable regressions in small cell lung cancers with high replication stress. Cancer Cell. Apr 12 2021;39(4):566–579.e7. doi:10.1016/j.ccell.2021.02.014 [PubMed: 33848478]
21. Pinyol R, Montal R, Bassaganyas L, et al. Molecular predictors of prevention of recurrence in HCC with sorafenib as adjuvant treatment and prognostic factors in the phase 3 STORM trial. Gut. Jun 2019;68(6):1065–1075. doi:10.1136/gutjnl-2018-316408 [PubMed: 30108162]
22. Chuah S, Lee J, Song Y, et al. Uncoupling immune trajectories of response and adverse events from anti-PD-1 immunotherapy in hepatocellular carcinoma. J Hepatol. Sep 2022;77(3):683–694. doi:10.1016/j.jhep.2022.03.039 [PubMed: 35430299]
23. Vogel A, Martinelli E, Vogel A, et al. Updated treatment recommendations for hepatocellular carcinoma (HCC) from the ESMO Clinical Practice Guidelines. Annals of Oncology. 2021;32(6):801–805. doi:10.1016/j.annonc.2021.02.014 [PubMed: 33716105]
24. Heimbach J, Kulik LM, Finn R, et al. Aasld guidelines for the treatment of hepatocellular carcinoma. Hepatology. Jan 28 2017;doi:10.1002/hep.29086
25. Fako V, Martin SP, Pomyen Y, et al. Gene signature predictive of hepatocellular carcinoma patient response to transarterial chemoembolization. Int J Biol Sci. 2019;15(12):2654–2663. doi:10.7150/ijbs.39534 [PubMed: 31754337]
26. Roessler S, Long EL, Budhu A, et al. Integrative genomic identification of genes on 8p associated with hepatocellular carcinoma progression and patient survival. Gastroenterology. 2012;142:957–966. NOT IN FILE. [PubMed: 22202459]
27. Lin Z, Niu Y, Wan A, et al. RNA m(6) A methylation regulates sorafenib resistance in liver cancer through FOXO3-mediated autophagy. Embo j. Jun 17 2020;39(12):e103181. doi:10.15252/embj.2019103181 [PubMed: 32368828]
28. Takai A, Dang H, Oishi N, et al. Genome-Wide RNAi Screen Identifies PMPCB as a Therapeutic Vulnerability in EpCAM(+) Hepatocellular Carcinoma. Cancer Res. May 1 2019;79(9):2379–2391. doi:10.1158/0008-5472.CAN-18-3015 [PubMed: 30862714]
29. Yang S-F, Chang C-W, Wei R-J, Shiue Y-L, Wang S-N, Yeh Y-T. Involvement of DNA Damage Response Pathways in Hepatocellular Carcinoma. BioMed Research International. 2014/04/28 2014;2014:153867. doi:10.1155/2014/153867 [PubMed: 24877058]
30. Lin P, Gao RZ, Wen R, He Y, Yang H. DNA Damage Repair Profiles Alteration Characterize a Hepatocellular Carcinoma Subtype With Unique Molecular and Clinicopathologic Features. Frontiers in immunology. 2021;12:715460. doi:10.3389/fimmu.2021.715460 [PubMed: 34456923]
31. Knijnenburg TA, Wang L, Zimmermann MT, et al. Genomic and Molecular Landscape of DNA Damage Repair Deficiency across The Cancer Genome Atlas. Cell Reports. 2018/04/03/2018;23(1):239–254.e6. doi:10.1016/j.celrep.2018.03.076 [PubMed: 29617664]
32. Goumard C, Desbois-Mouthon C, Wendum D, et al. Low Levels of Microsatellite Instability at Simple Repeated Sequences Commonly Occur in Human Hepatocellular Carcinoma. Cancer Genomics Proteomics. Sep-Oct 2017;14(5):329–339. doi:10.21873/cgp.20043 [PubMed: 28871000]
33. Lee JH, Hong J, Zhang Z, et al. Regulation of telomere homeostasis and genomic stability in cancer by N^6-adenosine methylation (m^6A). Science Advances. 2021;7(31):eabg7073. doi:doi:10.1126/sciadv.abg7073 [PubMed: 34321211]

34. Yin T, Zhao L, Yao S. Comprehensive characterization of m6A methylation and its impact on prognosis, genome instability, and tumor microenvironment in hepatocellular carcinoma. BMC Med Genomics. Mar 8 2022;15(1):53. doi:10.1186/s12920-022-01207-x [PubMed: 35260168]

35. Darè E, Zhang LH, Jenssen D, Bianchi V. Molecular analysis of mutations in the hprt gene of V79 hamster fibroblasts: effects of imbalances in the dCTP, dGTP and dTTP pools. Journal of molecular biology. Oct 6 1995;252(5):514–21. doi:10.1006/jmbi.1995.0516 [PubMed: 7563070]

36. Zhou W, Yao Y, Scott AJ, et al. Purine metabolism regulates DNA repair and therapy resistance in glioblastoma. Nature Communications. 2020/07/30 2020;11(1):3811. doi:10.1038/s41467-020-17512-x

37. Brown JS, O'Carrigan B, Jackson SP, Yap TA. Targeting DNA Repair in Cancer: Beyond PARP Inhibitors. Cancer Discovery. 2017;7(1):20–37. doi:10.1158/2159-8290.Cd-16-0860 [PubMed: 28003236]

38. Miller HA, Yin X, Smith SA, et al. Evaluation of disease staging and chemotherapeutic response in non-small cell lung cancer from patient tumor-derived metabolomic data. Lung Cancer. 2021/06/01/ 2021;156:20–30. doi:10.1016/j.lungcan.2021.04.012 [PubMed: 33882406]

39. Konstantinopoulos PA, da Costa AABA, Gulhan D, et al. A Replication stress biomarker is associated with response to gemcitabine versus combined gemcitabine and ATR inhibitor therapy in ovarian cancer. Nature Communications. 2021/09/22 2021;12(1):5574. doi:10.1038/s41467-021-25904-w

40. Barnieh FM, Loadman PM, Falconer RA. Progress towards a clinically-successful ATR inhibitor for cancer therapy. Current Research in Pharmacology and Drug Discovery. 2021/01/01/ 2021;2:100017. doi:10.1016/j.crphar.2021.100017 [PubMed: 34909652]

41. Wang Z, Ren Z, Chen Y, et al. Adjuvant Transarterial Chemoembolization for HBV-Related Hepatocellular Carcinoma After Resection: A Randomized Controlled Study. Clinical Cancer Research. 2018;24(9):2074–2081. doi:10.1158/1078-0432.Ccr-17-2899 [PubMed: 29420221]

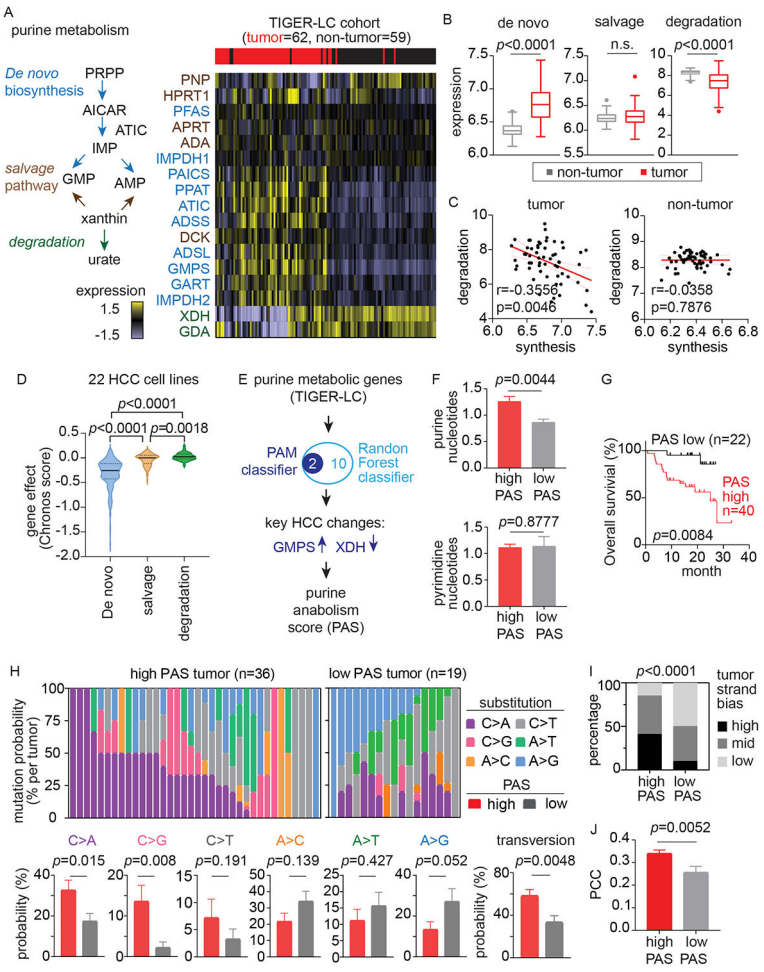

Figure 1: Reprogramming of purine metabolism is a recurrent event in HCC, linking to tumor biology and clinical aggressiveness.

(A) Heatmap summarizes the expression of purine metabolic genes in tumor and non-tumor tissues (TIGER-LC cohort, left panel), with a schema of purine metabolism shown on the left panel.

(B) Function changes of different components of purine metabolism in HCC and associated liver tissues. The boxplots summarize the distribution of the mean expression of indicated pathways in tumors and non-tumor tissues. The medium value is indicated by the middle line within box, and the 25th and 75th percentiles are indicated by the edges of box. The whiskers describe the ranged that is 1.5 time IQR more or less than the box and dots represent value that are greater or less than the range indicated by the whisker. Statistical significance is determined by two-sided independent t-test.

(C) The relationship of purine synthesis and purine degradation in HCC and associated liver tissues. Correlation coefficient and *p* values are based on two-sided Spearman's rank correlation coefficient test.

(D) Gene essentiality of purine metabolic genes. CRISPR-based gene essentiality score (representing as Chronos score) of 17 purine metabolic genes among 22 HCC cell lines were obtained from DepMap database[10] and summarized using violin plots. A lower Chronos

score indicates a gene is more likely to be dependent for cell fitness in a given cell line and a score of 0 indicates a gene is non-relevant for cell fitness.

(E) Development of purine anabolism score (PAS) to characterize purine metabolic status in HCC (Supplementary Table 1).

(F) PAS shows specificity in capturing associated metabolomic changes in HCC. The purine anabolic status of HCC tumors was defined based PAS, and the level of purine and pyrimidine nucleotides in high (n=40) and low (n=22) PAS tumors were compared. Bar, mean; error bars, S.D.; *p* values between high and low purine anabolic HCC tumors are calculated using two-sided independent t-test.

(G) Kaplan-Meier survival analysis of the 62 HCC patients based on the tumor PAS with two-sided log rank *p* value.

(H) Mutation substitution of HCC tumors with high- and low PAS in TIGER-LC cohorts (upper two panels). Each bar represents the substitution structure of a signal tumor. The collective probability of each substitution pattern is summarized below. Bar, mean; error bars, S.D.; *p* value between high and low PAS HCC tumors is calculated using two-sided independent t-test.

(I) Mutation strand asymmetry increases in high PAS HCC. The location of each mutation was identified using Mutalisk (Supplementary Fig.6), and the collective proportion of mutation occurring on transcribed strand to the untranscribed strand was used to define the degree of tumor strand bias (high =100%, mid =99-50%, low <50% of mutation occurring on the transcribed strand). The likelihood of different tumor strand bias in high and low PAS HCCs is compared using Chi-square test.

(J) High PAS HCCs show a significantly higher genomic complexity. Tumor genomic complexity was estimated using PCC value[11]. Bar, mean; error bars, S.D.; *p* value between high and low purine anabolic HCC tumors is calculated using two-sided independent t-test.

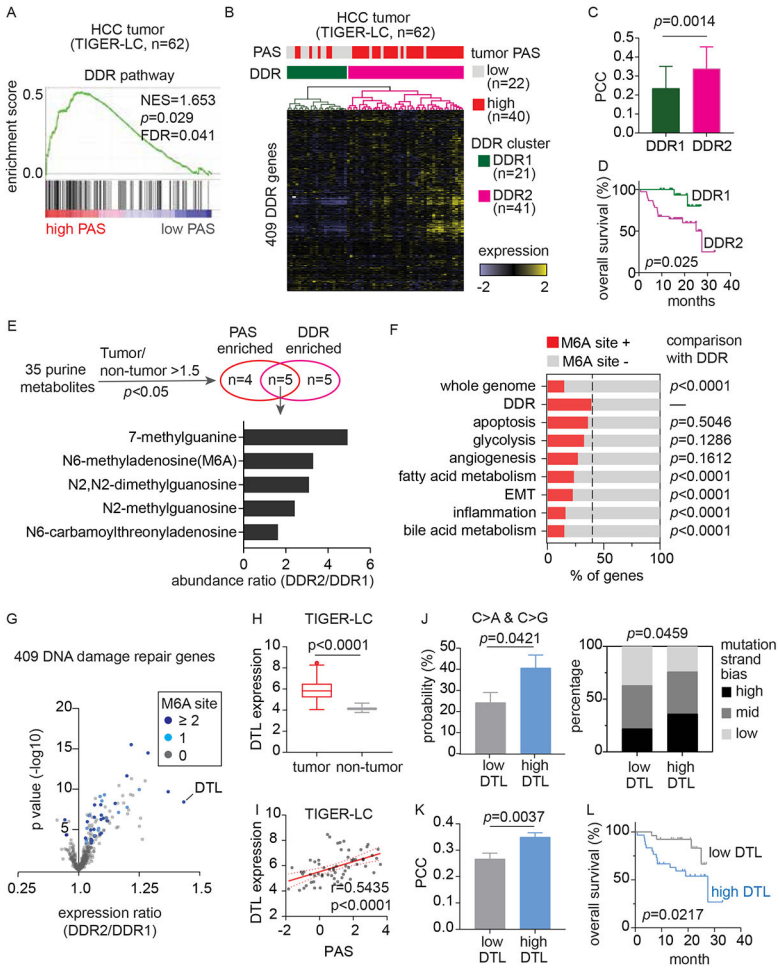

Figure 2: High tumor purine anabolism promotes dysregulation of DDR machinery through upregulating m^{6}A RNA modification.

(A) Dysregulation of DDR pathway is significantly associated with higher purine anabolism in HCC. Gene Set Enrichement Analysis was used to identify pathways significantly altered with the change of tumor purine anabolism in TIGER-LC cohort (Supplementary Table 3).

(B) Unsupervised hierarchical clusters of 409 DNA damage repair (DDR) genes shows high coincidence with tumor purine anabolic status. Heatmap summarizes the expression of DDR genes in HCC tumors with the annotation of DDR clusters and tumor PAS level shown on the top.

(C) Transcriptomic changes of DDR genes correlate with genomic complexity in HCC. Average PCC value was compared between DDR1 (n=21) and DDR2 (n=41) tumors using two-sided independent t-test. Bar, mean; error bars, S.D.

(D) Kaplan-Meier survival analysis of the HCC patients based on the tumor DDR status with two-sided log rank *p* value.

(E) Identification of purine metabolites that are concurrently enriched in high PAS tumors and DDR dysregulated tumors.

(F) The percentage of genes with m^{6}A modifying sites among different cancer hallmarks. The presence of m^{6}A modifying sites across human genome is obtained from WHISTLE[16]

and the percentage of m^6A + genes in DDR pathways is compared against that in whole genome and other cancer hallmark pathways using Fisher's exact test.
(G) DTL is identified for the presence of multiple m^6A modifying sites and the highest expressional changes driven by DDR dysregulation in HCC.
(H) The expressions of DTL in HCC and non-HCC liver tissues. Data is summarized using boxplots with the medium value is indicated by the middle line within box, and the 25^{th} and 75^{th} percentiles are indicated by the edges of box. summarize the distribution of the mean expression of DTL in tumors and non-tumor tissues. The whiskers describe the ranged that is 1.5 time IQR more or less than the box and dots represent value that are greater or less than the range indicated by the whisker. Statistical significance is determined by two-sided independent t-test.
(I) The association of DTL expressions and tumor purine anabolism in HCC tumors. Correlation coefficient and *p* value are based on two-sided Spearman's rank correlation coefficient test.
(J) Left panel: The probability of C>A and C>G substitution in HCC tumors with high (n=30) and low DTL (n=25). Bar, mean; error bar, S.D. Statistical significance is determined by two-sided independent t-test. Right pane: Mutational strand asymmetry in HCC tumors with high and low DTL. The distribution of tumor strand bias among high and low purine anabolic HCCs is compared using Chi-square test.
(K) The degree of genomic complexity in HCC tumors with high (n=33) and low (n=29) DTL. Bar, mean; error bar, S.D. Statistical significance is determined by two-sided independent t-test.
(L) Overall survival of HCC patients according to the expressions of DTL in tumor tissues. The survival significance is determined using a two-sided log-rank test.

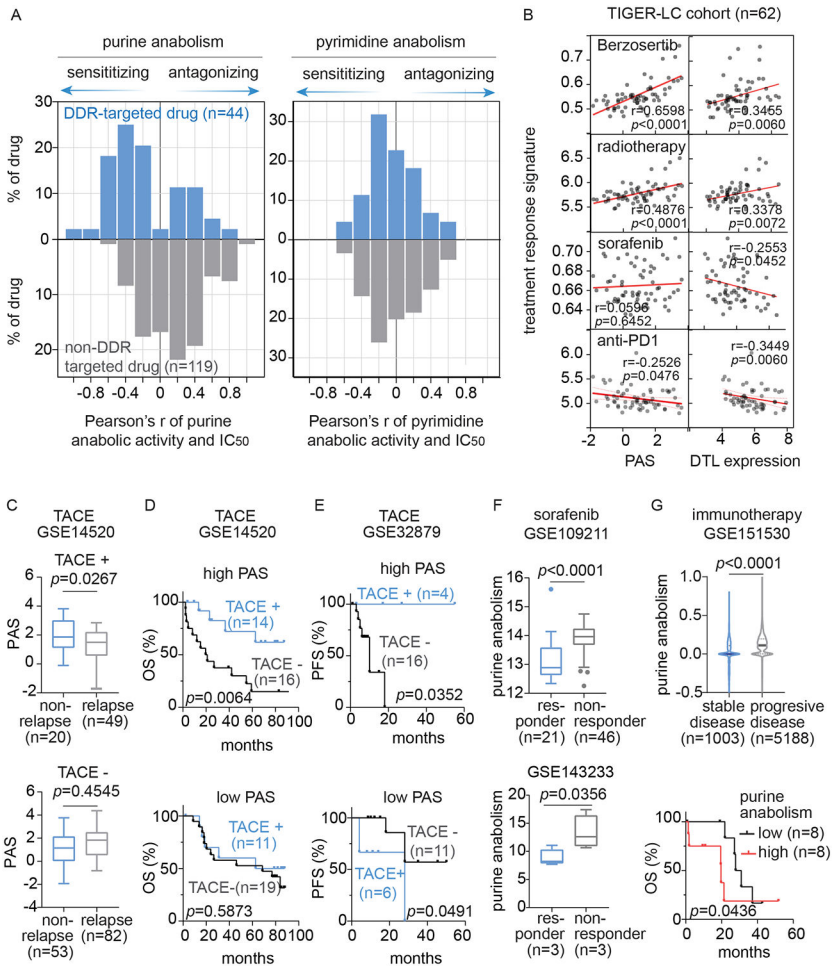

Figure 3. Activation of tumor purine anabolism creates therapeutic vulnerability to DDR targeting agents.

(A) The histogram summarizes the distribution of correlation coefficient linking therapeutic sensitivity to 180 targeted agents and tumor purine and pyrimidine anabolic status in 11 HCC cell lines. Dose response of drugs were obtained from Genomics of Drug Sensitivity in Cancer database and the status of purine and pyrimidine anabolism of cells lines were computed using the expression data obtained from Cancer Cell Line Encyclopedia. A negative correlation value suggests increasing purine or pyrimidine anabolism was associated with improving therapeutic sensitivity (lower IC_{50}), and vice versa.

(B) The relationship of drug response and purine anabolism score or tumor DTL level in HCC. Correlation coefficient and *p* value are based on two-sided Spearman's rank correlation coefficient test.

(C) Tumor purine anabolism score according to post-operative treatment and treatment response in the Chinese cohort. The minimum and maximum values are described by the extension of whiskers; the medium value is indicated by the middle line within box, and the 25th and 75th percentiles are indicated by the edges of box. Statistical significance is determined by two-sided independent t-test.

(D) Overall survival (OS) of advanced HCC patients receiving preventative TACE or observation according to tumor purine anabolic status in the Chinese cohort. The survival significance is determined using a two-sided log-rank test.
(E) Progression-free survival (PFS) of advanced HCC patients receiving preventative TACE or observation according to tumor purine anabolic status in the Korean cohort. The survival significance is determined using a two-sided log-rank test.
(F) HCC purine anabolic status according to sorafenib response. Data is summarized using boxplots with the medium value is indicated by the middle line within box, and the 25^{th} and 75^{th} percentiles are indicated by the edges of box. summarize the distribution of the mean expression of DTL in tumors and non-tumor tissues. The whiskers describe the ranged that is 1.5 time IQR more or less than the box and dots represent value that are greater or less than the range indicated by the whisker. Statistical significance is determined by two-sided independent t-test.
(G) Upper panel: Purine anabolic status of HCC cells according to immunotherapy response. Statistical significance is determined by two-sided independent t-test. Lower panel: Kaplan-Meier survival analysis of the HCC patients based on the tumor purine anabolic status with two-sided log rank *p* value.

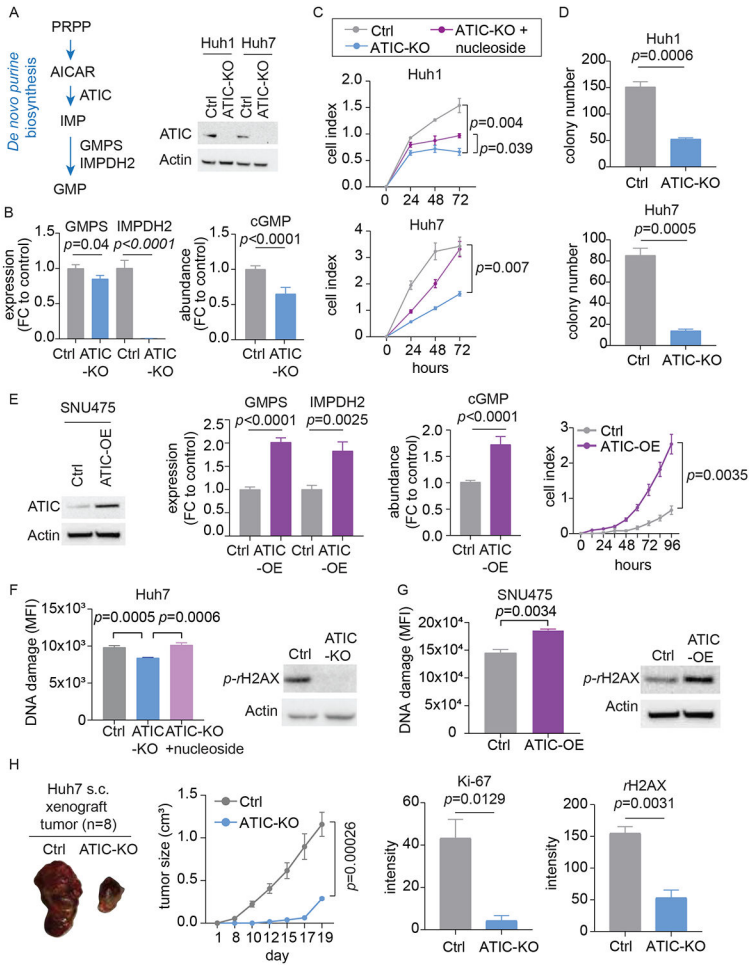

Figure 4. Activity of purine anabolism determines the proliferation and DNA damage in HCC

(A) Left panel summarizes the role of ATIC in purine *de novo* biosynthesis. Right panel: Validation of ATIC deletion in Huh1 and Huh7 cells.

(B) Validation of the effects of ATIC-knockout (KO) on inhibiting purine *de novo* biosynthesis. Bar plots summarize the levels of ATIC-downstream genes, namely GMPS and IMPDH2, and metabolite, namely cGMP, in control (Ctrl) and ATIC-KO Huh7 cells. (n=3) Bar, mean; error bar, S.D. Statistical significance is determined by two-sided independent t-test.

(C) The *in vitro* proliferation rates of Huh1 and Huh7 cells are significantly inhibited in cells with CRISPR-Cas9-mediated knockout of ATIC (ATIC-KO), which are reversed by supplement of nucleosides. (n=3) Dot, mean; error bar, S.D. Statistical significance is determined by two-sided independent t-test.

(D) The number of tumor colony formed by Huh1 and Huh7 cells with and without ATIC-KO. (n=3) Bar, mean; error bar, S.D. Statistical significance is determined by two-sided independent t-test.

(E) The *in vitro* proliferation rate of SNU475 cells is significantly enhanced by ectopic expression of ATIC (ATIC-OE). The effects of ATIC-OE in SNU475 cell are shown by the western blot (left), the levels of ATIC-downstream effectors (middle), and the cell

proliferation assay (right). (n=3) Bar and Dot, mean; error bar, S.D. Statistical significance is determined by two-sided independent t-test.

(F) ATIC-KO significantly decreases the level of DNA damage in Huh7 cells, while supplement of nucleosides counteracts with such effects. DNA damage of Huh7 cells is measured using flow cytometry (left panel) and the expression of *p*-r-H2AX (right panel). (n=3) Bar, mean; error bar, S.D. Statistical significance is determined by two-sided independent t-test.

(G) ATIC-OE increases the level of DNA damage in SNU475 cells. DNA damage of SNU475 cells is measured using flow cytometry (left panel) and the expression of *p*-r-H2AX (right panel). (n=3) Bar, mean; error bar, S.D. Statistical significance is determined by two-sided independent t-test.

(H) ATIC-KO significantly impairs *in vivo* growth of Huh7 xenografted tumor. Left two panel shows the picture of representative tumors and the growth curve of Huh7 xenograft tumors with and without ATIC-KO. (n=8) Right two panels show the quantified levels of proliferative maker, ki-67, and DNA damage marker, *p*-r-H2AX, in control and ATIC-KO tumors.

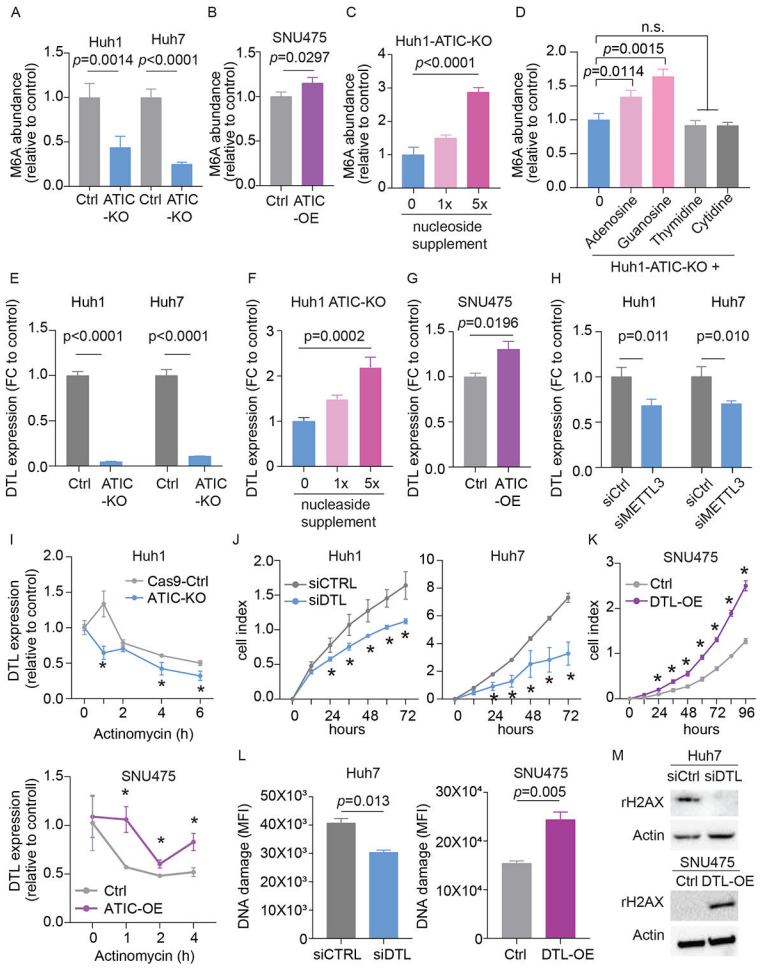

Figure 5. Purine anabolism regulates the level of m^{6}A RNA modification and DTL expression in HCC cells.

(A) The level of m^{6}A on RNA in Huh1 and Huh7 cells with and without ATIC-KO. (n=3) Bar, mean; error bar, S.D. Statistical significance is determined by two-sided independent t-test.

(B) The level of m^{6}A on RNAs in SNU475 cells with and without ATIC-OE. (n=3) Bar, mean; error bar, S.D. Statistical significance is determined by two-sided independent t-test.

(C,D) The level of m^{6}A-RNA in ATIC-KO Huh1 cell with supplement of pool nucleosides (C) or with supplement of individual nucleoside. (n=3) Bar, mean; error bar, S.D. Statistical significance is determined by two-sided independent t-test.

(E) The expression of DTL in Huh1 and Huh7 cells with and without ATIC-KO. (n=3) Bar, mean; error bar, S.D. Statistical significance is determined by two-sided independent t-test.

(F) The expression of DTL in ATIC-KO Huh1 cell with nucleoside. (n=3) Bar, mean; error bar, S.D. Statistical significance is determined by one-way ANOVA test.

(G) ATIC-OE significantly increases DTL expression in SNU475 CELLS. Bar, mean; error bar, S.D. Statistical significance is determined by two-sided independent t-test.

(H) Inhibition of METTL3, a key m^{6}A-associated methyltransferase, significantly decreases the expression of DTL in Huh1 and Huh7 cells. (n=3) Bar, mean; error bar, S.D. Statistical significance is determined by two-sided independent t-test.

(I) The stability of DTL gene is affected by purine anabolic activity in HCC. Huh7 cells with and without ATIC-KO (upper panel) and SNU475 cells with and without ATIC-OE were exposed to actinomycin treatment and harvested at indicated time point for assessments of DTL expression. Dot, mean; error bar, S.D. Statistical significance is determined by two-sided independent t-test. *, p value <0.05.

(J) DTL knockdown significantly inhibits the proliferation rate of Huh1 and Huh7 cells. Dot, mean; error bar, S.D. Statistical significance is determined by two-sided independent t-test. *, p value <0.05.

(K) DTL overexpression significantly enhance the proliferation rate of SNU475 cells. Dot, mean; error bar, S.D. Statistical significance is determined by two-sided independent t-test. *, p value <0.05.

(L, M) DTL regulates cellular DNA damage in HCC. The level of DNA damage lesions (L) and the expressions of p-r-H2AX were accessed in Huh7 cells with and without ATIC-KO and in SNU475 cells with and without ATIC-OE. (n=3) Bar, mean; error bar, S.D. Statistical significance is determined by two-sided independent t-test.

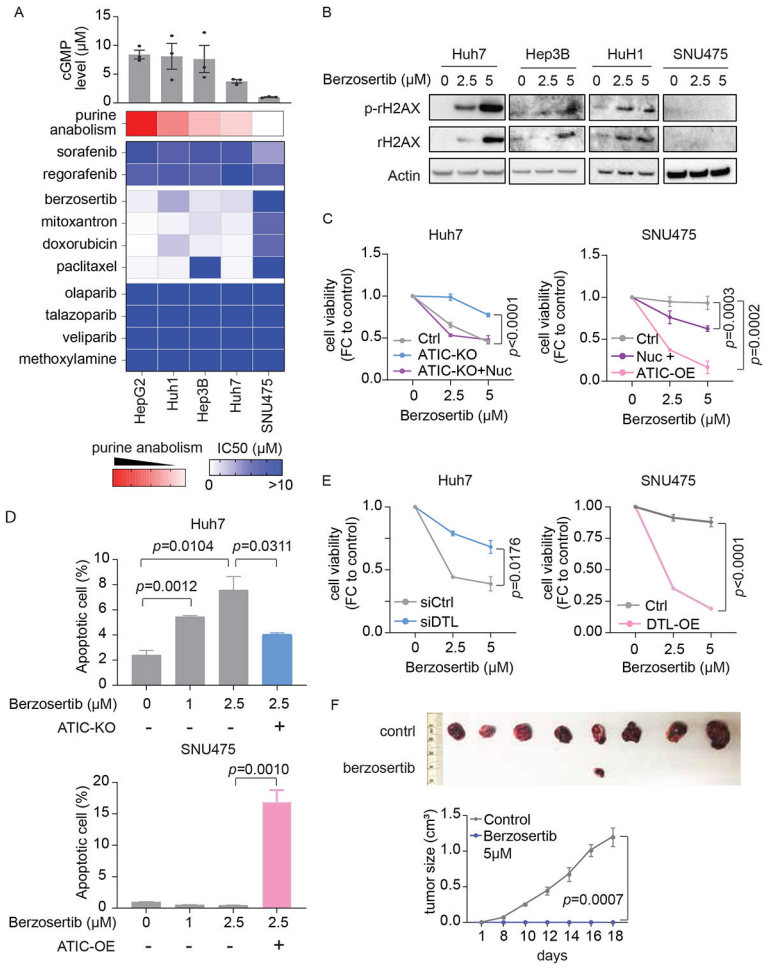

Figure 6. Activation of purine anabolism creates therapeutic vulnerability towards compounds targeting double strand break repair.

(A) Purine anabolic status determines the *in vitro* therapeutic susceptibility of HCC cells. Five HCC cell lines were treated with two clinical-approved HCC target therapies (sorafenib and regorafenib), five target therapies against DDR pathways (berzosertib, olaparib, talazoparib, veliparib and methoxyamine), and three DNA damaging chemotherapies that were known to induce double strand break (mitoxantrone, doxorubicin and paclitaxel). Purine anabolic activities of HCC cell lines were estimated by the abundance of cGMP (top panel) and the average expression of purine anabolic genes (CCLE database, middle panel). Drug IC_{50} of indicated cell lines were determined after 48 hours of treatment and summarized in the heatmap (lower panel).

(B) Berzosertib treatment increases cellular DNA damage in a dose dependent manner specifically in HCC cells with high purine anabolism. Representative western blot images show the expression of *p*-r-H2AX and r-H2AX in HCC cells treated with berzosertib.

(C) Purine anabolic activity regulates the cytotoxic effects of berzosertib in HCC cells. The viabilities of Huh7 cells with and without ATIC-KO and the viabilities of SNU475 cells with and without ATIC-OE after exposing to indicated treatments for 48 hours were accessed. Dot, mean; error bar, S.D. Statistical significance is determined by two-sided independent t-test.

(D) Purine anabolic activity determines the pro-apoptotic effects of berzosertib in HCC. Hun7 cell with and without ATIC-KO and SNU475 cells with and without ATIC-OE were treated with berzosertib at indicated doses for 48 hours and harvested for flow cytometry analysis. Apoptotic cells are characterized by positive expression of Annexin V but negative for PI staining. Bar, mean; error bar, S.D. Statistical significance is determined by two-sided independent t-test.

(E) DTL expression determines the effects of berzosertib. in HCC. Hun7 cell with/without DTL-KD and SNU475 cells with/without DTL-OE were treated with berzosertib at indicated doses for 48 hours and examined for cell viability. Dot, mean; error bar, S.D. Statistical significance is determined by two-sided independent t-test.

(F) Berzosertib treatment significantly abolishes the *in vivo* tumor growth of Huh7 xenografted tumor. Huh7 cells were treated with control or berzosertib 5μM for 48 hours before implantation. $1x10^6$ post-treatment viable cells were injected subcutaneously to mice and tumor growth was observed for three weeks. Upper panel shows the picture of tumors and lower panel shows the growth curve of Huh7 tumor. (n=8) Dot, mean; error bar, S.D. Statistical significance is determined by two-sided independent t-test.